Self-adhesion of uncrosslinked poly(butadiene- co -acrylonitrile), i.e. nitrile rubber, an inhomogeneous and associative polymer

Valentine Hervio, Annie Brûlet, Costantino Creton, Gabriel E Sanoja

ARTICLE

Self-Adhesion of Uncrosslinked Poly (butadiene-co-acrylonitrile), i.e. Nitrile Rubber, an Inhomogeneous and Associative Polymer

Received 00th January 20xx,
Accepted 00th January 20xx

DOI: 10.1039/x0xx00000x

Valentine Hervio[a], Annie Brûlet[b], Costantino Creton[a,*], and Gabriel E. Sanoja[a,†,*]

Nitrile rubber (i.e., NBR) is a crosslinked copolymer of butadiene and acrylonitrile that finds widespread use in the automotive and aerospace industry as it sustains large, reversible deformations while resisting swelling by petrochemical fuels. We recently demonstrated that this material has a drift in composition due to the difference in reactivity between acrylonitrile and butadiene monomers during emulsion copolymerisation. Thus, although NBR is often thought of as a random copolymer, it does experience thermodynamic driving forces for self-assembly and kinetic barriers for processing like those of block copolymers.[1] Here, we illustrate how such drift in composition hinders interdiffusion and prevents self-adhesion. The key result is that contacting uncrosslinked NBR (i) in the melt, (ii) in the presence of tackifiers, or (iii) in the presence of organic solvents promotes interdiffusion and enables self-adhesion. However, the contact times required for self-adhering, $t_c \sim O($100 h$)$, are still orders of magnitude above those needed for non-polar synthetic rubbers like styrene-butadiene rubber (i.e., SBR) of comparable molecular weights and glass transition temperatures, $t_c \sim O($100 s), unveiling the dramatic effect of compositional inhomogeneities and physical associations on polymer interdiffusion and large-strain mechanical properties. For example, when welded with organic solvents, the self-adhesion energy of NBR continues to increase after the solvent has evaporated because of polymer nanostructuring effects.

Introduction

Polar elastomers find widespread use in automotive and aerospace applications because of their ability to sustain large, elastic, and reversible deformations while resisting swelling by non-polar fuels like gasoline, motor oil, and kerosene. One of the most important polar elastomers, nitrile rubber or NBR, dates to the early 1930s when IG Farben chemists Erich Konrad and Eduard Tschunkur synthesised a series of poly(acrylonitrile-*co*-butadiene) copolymers by emulsion polymerisation in water. Since then, these copolymers have been crosslinked, and NBR has become a large-volume synthetic rubber with bulk properties that can be readily tailored through the acrylonitrile content, 18 to 40 wt%.

A classic strategy to form NBR into complex objects or parts is to assemble multiple raw, uncrosslinked, and tacky polymer layers, wait for some contact time, and then crosslink. This strategy is used in manufacturing rubber tyres with poly(styrene-*co*-butadiene) copolymers. It requires sufficient tack or self-adhesion between the polymer layers to mitigate the nucleation of structural defects (*i.e.*, cracks) that progressively grow until failure. Examples of NBR parts are not as well-known as rubber tyres, but they include flexible fuel tanks and hoses in the automobile and aviation sectors.

Due to its importance for the mechanical lifetime of synthetic elastomers or rubbers, the interdiffusion and self-adhesion of uncrosslinked polymer layers have been previously investigated.[2–9] For example, in a seminal investigation on non-polar, narrowly dispersed, and compositionally homogeneous poly(styrene-*co*-butadiene), the precursor of styrene-butadiene rubber or SBR, Schach *et al.* illustrated that the process of self-adhesion is governed by polymer interdiffusion; and the associated self-adhesion energy, W_{adh}, by two dimensionless groups: (i) the ratio of the contact time, t_c, to the polymer reptation time, τ_d, and (ii) the ratio of the reptation time, τ_d, to the debonding time, h_0/V_d, referred to as the Deborah number, De.[10] Here, V_d is the debonding speed and h_0 the initial thickness of the adhesive layer. At room temperature, non-polar elastomers like SBR or natural rubber typically require contact times, $t_c \sim O($100 s$)$, to self-adhere to the level of bulk cohesive strength.[10,11] However, polar elastomers like NBR require drastically larger contact times, $t_c \sim O($100 h$)$, despite having a similar glass transition temperature, T_g, suggesting that these materials may have a more significant kinetic barrier for polymer interdiffusion and self-adhesion.[11]

We recently shed some light on the dynamics of uncrosslinked and industrial-grade NBR, demonstrating that it can be mechanically rejuvenated and physically aged due to an inhomogeneous distribution of acrylonitrile and butadiene monomers along the polymer chains.[1] Namely, uncrosslinked NBR is constituted of blocks of poly(butadiene) and poly(acrylonitrile-*alt*-butadiene) as a result

[a] *Laboratoire Sciences et Ingénierie de la Matière Molle, ESPCI Paris, Université PSL, CNRS UMR 7615, Sorbonne Université, 75005, Paris, France.*
[b] *Laboratoire Léon Brillouin, UMR 12 CEA-CNRS, Université Paris Saclay, 91191, Gif-sur-Yvette, France.*
†Present address: McKetta Department of Chemical Engineering. 200 E Dean Keeton St. Austin, TX 78712-1589. USA.
*Correspondence to G.E.S (gesanoja@che.utexas.edu) and C.C (costantino.creton@espci.psl.eu)
Electronic Supplementary Information (ESI) available: [details of any supplementary information available should be included here]. See DOI: 10.1039/x0xx00000x

of the difference in reactivity ratios between acrylonitrile and butadiene during emulsion copolymerisation. Such inhomogeneous distribution of monomers along the polymer chains results in thermodynamic driving forces for microphase separation and kinetic barriers for thermal- and solvent-processing like those of block copolymers;[12–17] a behaviour that contrasts that of compositionally homogeneous copolymers like SBR. Hence, extruding NBR at high temperature and shear results in a weakly microphase separated nanostructure of short reptation time and low resistance to flow, whereas physically ageing NBR leads to lamellar nanodomains, more solid-like properties and much slower stress relaxation. This effect of processing on NBR's nanostructure and viscoelastic properties translates into a time-dependent reptation time with important consequences on polymer interdiffusion and self-adhesion. Here, we aim to fundamentally understand such consequences to aid the design and engineering of rubber parts based on polar elastomers.

To understand the role of compositional inhomogeneities on polymer interdiffusion and self-adhesion, we put in contact two layers of an industrial-grade, uncrosslinked, and high molecular weight NBR over a range of temperatures for 1 h and, at room temperature over a range of contact times in the presence of tackifiers or organic solvents. The resulting interfaces were then debonded with a modified probe test, and the evolution of the self-adhesion energy with contact time was rationalised by considering the nanostructure and viscoelastic properties of the polymer, as well as the time scale of diffusion and evaporation of the organic solvent. This work provides a molecular picture of why polar elastomers like NBR require significant contact times, $t_c \sim O(100\ \text{h})$, to attain their cohesive strength during self-adhesion.

Experimental Section

Materials: Uncrosslinked, stabilised, and industrial-grade NBR with an average acrylonitrile content of 33 mol% was provided by Sidiac. 1H NMR did not detect trace impurities from the industrial copolymerisation of acrylonitrile and butadiene. GPC was only conducted in 80 wt% of the polymer and revealed a weight average molecular weight, M_w, of 127 kDa and a dispersity index of 2 (see trace in **Fig. S1**). The remainder 20 wt% had a M_w > 400 kDa and was outside the range of the columns. **Differential Scanning Calorimetry:** Thermograms were collected on a TA Instruments G200 at 20 °C/min between -150 °C and 120 °C, and the glass transition temperature T_g was determined from the midpoint method.

X-Ray Scattering: Scattering patterns were collected at the Laboratoire Léon Brillouin (CEA Saclay) on a Xenocs-Xeuss 2.0 equipped with a Pilatus detector. The X-ray source was a copper anode with Kα radiation of wavelength 1.54159 Å. The sample-to-detector distance was manually adjusted from 15 cm to 2.5 m, the aperture of scatterless slits was adapted to the appropriate q-range, and the 2D scattering patterns were azimuthally integrated to generate 1D scattering profiles. Empty beam and electronic backgrounds (*i.e.*, dark) were subtracted with a previously established procedure[18] and master curves were constructed by superimposing 1D scattering profiles collected over different q ranges.

Specimen Preparation: NBR was heat pressed at 100 °C and 50 bar for 1 h and then cooled to room temperature at 50 bar for 1 h. Rheology specimens were punch-cut with an 8 mm diameter, whereas dog bone specimens were punch-cut with a 5 mm wide and 20 mm gauge length. All samples had a thickness of approximately 2 mm.

Rheology: The rheological properties of NBR were determined with an Anton Paar MCR501 rheometer. Frequency sweeps from 0.01 Hz to 30 Hz at 25 °C and 60 °C were performed within the linear viscoelastic regime at a strain of 0.2%. Master curves were constructed using a reference temperature of 25 °C, and vertical and horizontal shift factors.

Tensile Tests: NBR was uniaxially deformed on an Instron 3343 equipped with a 10 N load cell. A constant crosshead speed of 0.33 mm/s (initial nominal strain rate $\dot{\varepsilon} = 0.02\ \text{s}^{-1}$) was imposed, and the resulting strain was determined from the crosshead position.

Solvent-Casting of NBR into Thin Films: Glass slides were cleaned with acetone, coated with hydroxyl groups by plasma treatment, and allowed to react with 3-(mercaptopropyl)-trimethoxysilane for 3 h at room temperature under vacuum.

NBR was dissolved in cyclohexanone (2.5 wt%), and the resulting solution was drop cast as a uniform layer on a silanised glass slide by drying first for 15 h at room temperature and atmospheric pressure and then for 2 h at 100 °C under vacuum. The resulting NBR layer had a thickness of approximately 5 μm. It was well-adhered to the substrate due to the thiol-ene click reaction between the mercapto groups on the glass slide and the alkene groups on the polymer backbone.

Heat-Pressing of NBR into Thick Films: NBR was heat-pressed in a rectangular mould (1.5 cm width and 6 cm length) at 100 °C and 50 bar for 1 h and then cooled to room temperature at 50 bar for 1 h. The mould's top and bottom were covered with a silicone release liner to avoid adhesion between NBR and the hot plates. After cooling, probe-tack specimens were punch-cut with an 8 mm diameter and 500 μm thickness, h_0.

Probe-Tack Tests: The self-adhesion properties of NBR were determined with a probe-tack setup mounted on a hydraulic MTS 810 tensile tester equipped with a 2 kN load cell and described in detail in Lakrout *et al.*[19] However, because of the prolonged contact times needed for self-adhesion, the procedure had to be adapted to decouple the bonding and debonding conditions.

Specifically, the NBR-NBR interface was formed outside the probe-tack setup, putting in contact thin (*ca.* 5 μm) and thick (*ca.* 500 μm) NBR layers first at a nominal contact pressure of 0.3 MPa for 1 h and then in the absence of a load for a contact time, t_c, at room temperature. The resulting glass-thin NBR-thick NBR assemblies were then mounted on the probe-tack setup, glueing the back of the thick NBR layer to a steel probe with cyanoacrylate Loctite 406 glue. The probe was pulled at a constant debonding speed, V_d, of 10 μm/s (initial nominal strain rate $\dot{\lambda} = 0.02\ \text{s}^{-1}$) to assess the adhesion of the NBR-NBR interface.

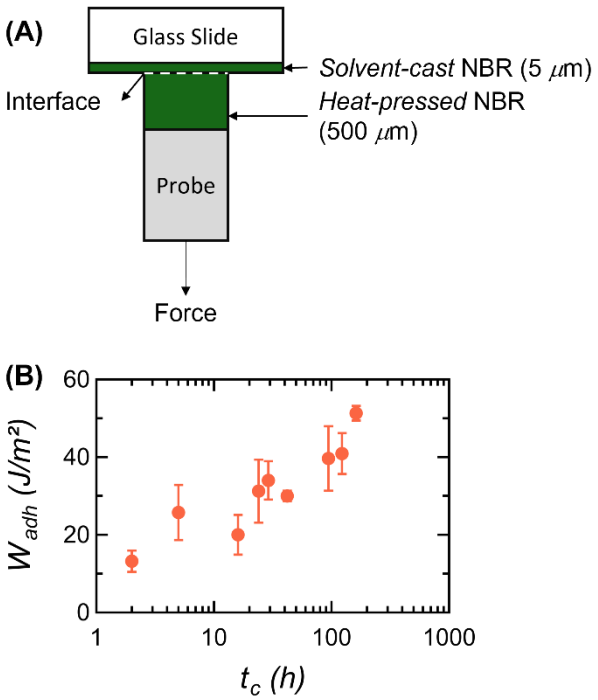

Figure 1. Self-adhesion of NBR. (**A**) Schematic of a probe-tack test. *Solvent-cast* NBR has a lamellar nanostructure whereas *heat-pressed* NBR is weakly microphase separated. (**B**) Evolution of the self-adhesion energy with contact time upon contacting and debonding at room temperature.

Again, this methodology is adapted from conventional probe-tack tests,[20–22] and is advantageous because it enables (i) polymer interdiffusion and self-adhesion over long contact times and (ii) decoupling of the bonding and debonding conditions.

Cross-linking of NBR: Uncrosslinked NBR was masticated with 2.4 phr of dicumyl peroxide at 85 °C for 20 min in a twin-screw extruder and then heat pressed at 150 °C for 2 h in a mould of thickness ≈ 2 mm.

Equilibrium Swelling of NBR: Crosslinked NBR was punch-cut into specimens of 8 mm diameter and 2 mm thickness and swollen to equilibrium in scintillation vials filled with organic solvent. The swelling ratio, *Q*, was determined with the following equation:

$$Q = 100\left(\frac{m_f - m_0}{m_0}\right)$$

Where m_0 and m_f are the initial and final mass of the specimen, respectively.

Results and Discussion

"Self-Adhesion" of NBR

We evaluated the self-adhesion energy of NBR by conducting probe-tack tests on adhesive layers that result from contacting *solvent-cast* and *heat-pressed* NBR under conditions like those encountered in industrial sites. However, it is worth noting that *solvent-cast NBR* was solvent-cast from a concentrated polymer solution (2.5 wt% in cyclohexanone), and *heat-pressed NBR* was

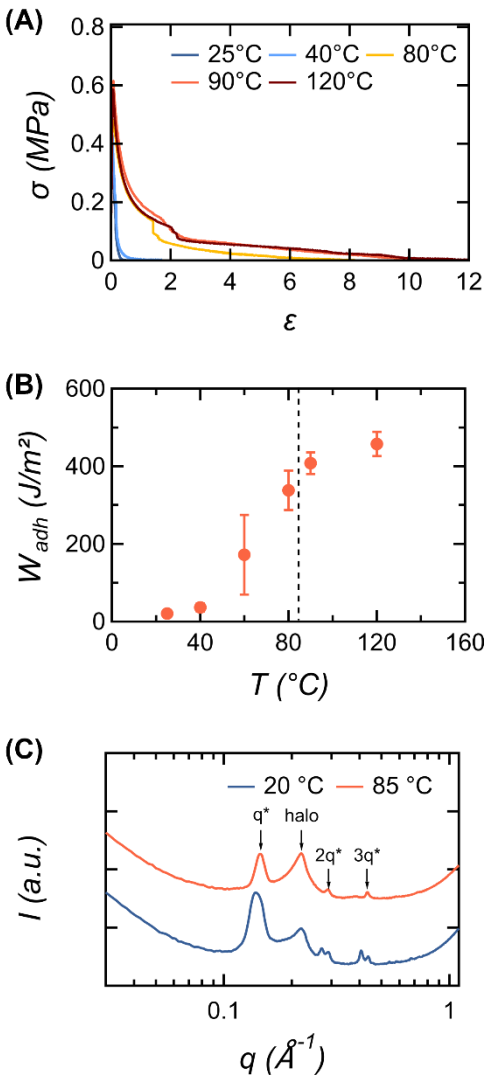

heat-pressed at high temperature and pressure. Thus, their nanostructures and viscoelastic properties might differ. Solvent casting NBR leads to a lamellar phase (LAM) of experimentally inaccessible reptation time, $\tau_d > 2500$ s, whereas heat-pressing NBR presumably results in a weakly microphase separated nanostructure (AGG) with a shorter reptation time (see Fig. S3 as

Figure 2. Effect of contact temperature on the self-adhesion of NBR. (**A**) Probe-tack test of NBR. Stress-strain curves (V_d = 10 μm/s; t_c = 1 h) reveal a transition in the failure mechanism from interfacial crack propagation to bulk fibril elongation at $T \approx 80$ °C, near the glass transition temperature $T_g \sim 75$ °C. This transition results in an (**B**) increase in the self-adhesion energy W_{adh} from 20 J/m^2 at 25 °C to 460 J/m^2 at 120 °C. It is attributed to melting poly(acrylonitrile-*alt*-butadiene) glassy domains at T_g (dashed line) and deterred short-range order. (**C**) X-ray scattering profiles illustrate the broadening of the high-order peaks at $q/q^* = 2$ and $q/q^* = 3$, supporting this picture. Details on the nanostructure are discussed in Hervio *et al.*[1]

adapted from Hervio *et al.*).[1] As a result, the polymer chains of solvent-cast NBR cannot interdiffuse even when contacted at room temperature for a long time. The self-adhesion energy moderately increases to $W_{adh} \approx 50$ J/m^2 after $t_c \sim 100$ h (**Fig. 1**). Interestingly, this W_{adh} is far from the bulk cohesive strength, $W_{coh} \sim O(10$ kJ/m^2),[11] an observation that we attribute to the slow reptation and interdiffusion that results from microphase separation into poly(acrylonitrile-*alt*-butadiene) and poly(butadiene) domains.

Case I: Short Contact Times at High Temperature

To overcome the kinetic barriers for polymer interdiffusion, *heat-pressed* and *solvent-cast* NBR were brought in contact first at 0.3 MPa for 1 h at room temperature and then *in the absence of a load for 1 h at temperatures ranging from 25 to 120 °C*. The resulting glass-NBR-NBR assemblies were then mounted on a probe-tack setup and debonded at a constant speed, $V_d \approx 10$ μm/s (initial nominal strain rate $\dot{\varepsilon} = 0.02$ s^{-1}), at room temperature.

The stress-strain curves of the probe tack tests are presented in Fig. 2A and reveal a sudden improvement in self-adhesion at $T \approx 80$ °, with a two-step drop in stress at a critical strain, $\varepsilon \approx 2$, associated with walls between cavities collapsing and fibrils forming.[23,24] At temperatures below 80 °C, the reptation time is comparable to the contact time, $\tau_d \sim O(1\text{ h})$, and the adhesive fails by interfacial crack propagation. In contrast, at temperatures above 80 °C, the reptation time is short relative to the contact time, $\tau_d \sim O(10\text{ s})$, and the adhesive fails in the bulk by fibril elongation. This observation is analogous to that reported by Schach *et al.* in highly entangled SBR subject to debonding above a critical Deborah number $De_{crit} \sim 3$,[10] and consistent with the increase in self-adhesion energy W_{adh} with contact temperature T from 20 J/m^2 at 25 °C to 460 J/m^2 at 120 °C in Fig. 2B.

X-ray scattering profiles in Fig. 2C and differential scanning calorimetry in Fig. S2 reveal that heating NBR from 20 to 85 °C, near the glass transition temperature T_g of the poly(acrylonitrile-*alt*-butadiene) domains, leads to a broadening of the higher-order scattering peaks and a disruption of the short-range order. Hence, contacting NBR in the melt (*i.e.*, $T > T_g$) affects the nanostructure and likely facilitates polymer interdiffusion by increasing (i) the thermal energy k_BT relative to the binding energy E_B of the dipole-dipole interactions between the acrylonitrile units (*i.e.*, stickers) and (ii) the segmental mobility of the polymer chains. Such diffusion of NBR as an inhomogeneous polymer melt is analogous to that reported by Feldman *et al.* in triblock copolymers with hydrogen-bonded 2-ureido-4[1H]-pyrimidinone (UPy) units confined to the end blocks,[25] and responsible for the increase in self-adhesion energy with contact temperature. However, it is worth noting that facilitating polymer interdiffusion by contacting NBR in the melt only leads to moderate enhancements in self-adhesion energy, W_{adh}, motivating other strategies to attain interfaces as strong as the bulk cohesive strength.

Case II: Long Contact Times in the Presence of Tackifiers

Another strategy to overcome the kinetic barriers for polymer interdiffusion is to co-extrude NBR with *tackifiers that selectively screen either the polar dipole-dipole or the non-polar hydrophobic interactions.* These tackifiers are phenolic in nature and incorporated at low concentrations, 3 wt%, such that the glass transition temperature $T_g \approx -30$ °C, complex storage G' and loss G'' moduli, and mechanical properties under uniaxial elongation are just like that of a control NBR extruded without tackifier (at least at the strains relevant for self-adhesion, $\varepsilon < 4$, Fig. S4-S5). NBR with and without tackifier was *solvent-cast* into slides and brought in contact with *heat-pressed* NBR first at 0.3 MPa for 1 h at room temperature, then *in the absence of a load at room temperature*

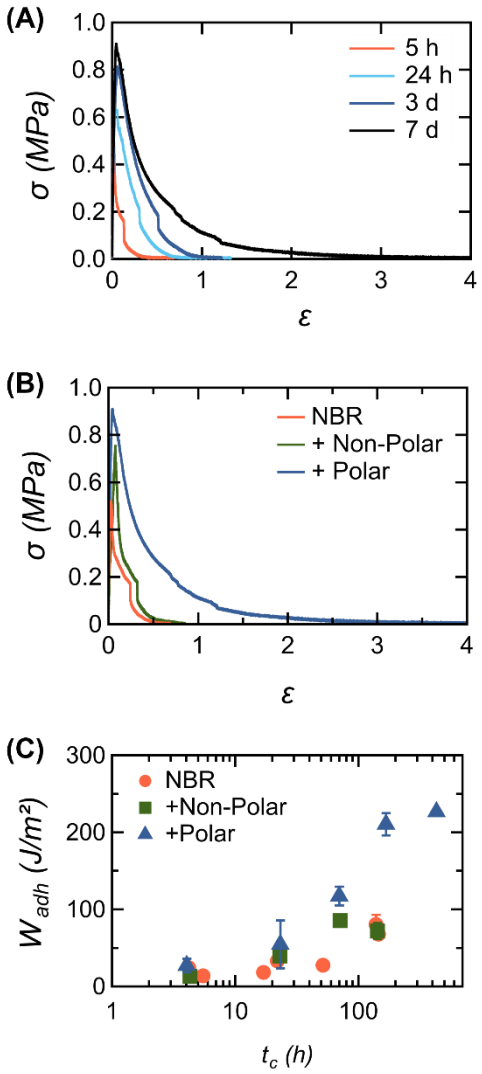

Figure 3. Effect of tackifier polarity on the self-adhesion of NBR. (**A**) Probe-tack test of NBR. Stress-strain curves reveal a transition in the failure mechanism from interfacial crack propagation to bulk fibril elongation at a contact time $t_c \approx 24$ h for the NBR containing 3 wt% polar tackifier. The (**B**) stress-strain curves after $t_c \approx 7$ days reveal that this polymer is more self-adhered, consistent with an (**C**) increase in the self-adhesion energy W_{adh} from 27 J/m^2 at 4 h to 225 J/m^2 that is attributed to more effective polymer interdiffusion due to screened dipole-dipole interactions.

over a range of contact times, t_c. The resulting glass-NBR-NBR assemblies were then mounted on a probe-tack setup and debonded at a constant speed, V_d = 10 μm/s (initial nominal strain rate $\dot{\varepsilon}$ = 0.02 s^{-1}), at 25 °C.

The stress-strain curves in Fig. 3A reveal the evolution of the failure mechanism with contact time t_c. At short contact times, t_c < 24 h, polymer self-diffusion is too slow to form a robust interface, and the adhesives fail by interfacial crack propagation; whereas at long contact times t_c > 24 h, polymer self-diffusion of the NBR co-extruded with polar tackifier is fast enough to form a somewhat robust interface. The adhesive fails by formation and elongation of fibrils. This transition in the failure mechanism in NBR co-extruded with polar tackifier is associated with an increase in the self-adhesion energy, W_{adh}, from 27 to 225 J/m^2 after 432 h (*i.e.*, 7 days) in Fig. 3B, and is challenging to rationalise considering the insensitivity of the linear and non-linear mechanical properties to the concentration and polarity of the tackifier.

We suggest two plausible explanations for this behaviour. The first one relates to the dynamics of the inhomogeneous and associative polymers. In this regard, it is worth noting that NBR, though characterised by an inhomogeneous distribution of acrylonitrile and butadiene monomers along the polymer chains, is also constituted of an ensemble of polymer chains with different compositions. After all, the propagation and termination of the polymer chains during emulsion copolymerisation are stochastic. Hence, it is possible for the non-polar tackifier to be inconsequential for the polymer dynamics and for the polar tackifier to screen the dipole-dipole interactions and facilitate polymer interdiffusion. This latter effect, however, is expected to notably depend on whether the chains resemble more random or blockier copolymers and only to affect a fraction of the polymer chains sufficiently small not to impact the complex moduli, *G'* and *G"* (*i.e.*, not representative of the ensemble average).[13,26–29]

The second explanation is temporal and relates to the evolution of the nanostructure and linear viscoelastic properties upon mechanical rejuvenation and physical ageing. Co-extruding NBR leads to a weakly segregated nanostructure of low relaxation time and resistance to flow that physically ages into lamellae of more solid-like character (see X-ray scattering profiles and estimates of the relaxation time in Hervio *et al.*,[1] Fig. 2 and 6). This mechanical rejuvenation and physical ageing leads to a time-dependent reptation time that introduces an additional timescale in the process of self-adhesion. When the polar tackifier screens the dipole-dipole interactions in the freshly extruded, heat-pressed, and mechanically rejuvenated NBR, the polymer chains inter-diffuse more effectively before ageing, forming a more robust interface. However, when the non-polar tackifier screens the hydrophobic interactions, the polymer chains' dynamics will likely be unaffected because of the low binding energy E_b relative to k_BT.

Case III: Contacting for Long Times in the Presence of Solvent

A typical industrial practice to enhance the self-adhesion of uncrosslinked rubbers is to clean and weld the contact surfaces (*i.e.*, interfaces) with solvent. Although this process is widespread in forming NBR into objects and parts, guidelines to choose the best solvent based on the molecular mechanism responsible for promoting adhesion remain elusive. Hence, we welded *solvent-cast* and *heat-pressed* NBR in the presence of solvents of varying polarity (and boiling point) by depositing 3 μL of solvent on 25 μL of *heat-pressed* NBR, putting in contact *solvent-cast* NBR for 1 h at 0.3 MPa and room temperature, and *allowing the interface to form in the absence of a load at room temperature over a range of contact times, t_c*. The self-adhesion energy, W_{adh}, was then investigated by debonding at a constant speed, V_d = 10 μm/s, with a probe-tack test at 25 °C.

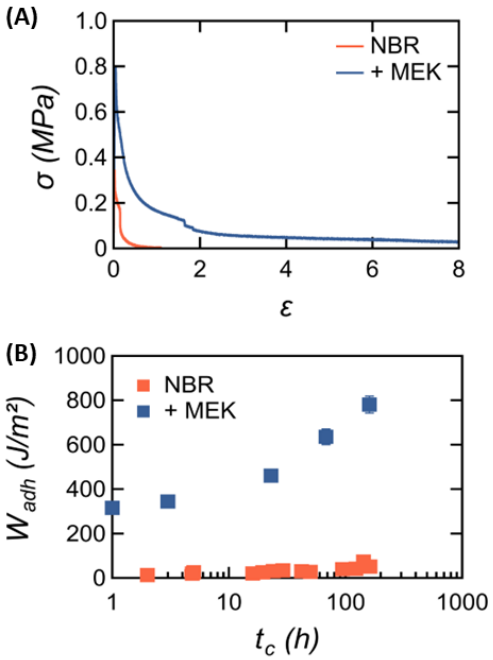

The stress-strain curves in Fig 4A and the evolution of W_{adh} with t_c in Fig. 4B unveil a dramatic improvement in the self-adhesion energy upon welding with methyl ethyl ketone (MEK). This observation indicates that contacting NBR in the presence of a polar solvent like MEK accelerates polymer interdiffusion and promotes self-adhesion by (i) screening the dipole-dipole interactions between the acrylonitrile monomers and (ii) facilitating segmental motion of the polymer chains. Such formation of an interface where the polymer chains become entangled leads to notable dissipation of elastic energy by fibril elongation until failure upon debonding and is consistent with previous observations on immiscible polymer melts [30] and polymer glasses.[31,32] In addition, it is similar to that observed when contacting at high temperature (Case I) or in the presence of a polar tackifier (Case II), highlighting the importance of overcoming dipole-dipole interactions to promote molecular interdiffusion and attaining a reasonable level of NBR self-adhesion.

Figure 4. Effect of methyl ethyl ketone (MEK) on the self-adhesion of NBR. (**A**) Probe-tack test of NBR. Stress-strain curves reveal a transition in the failure mechanism from interfacial crack propagation to bulk fibril elongation upon welding with MEK. This transition results in an (**B**) increase in the self-adhesion energy from 315 to 780 J/m^2 over 160 h.

Another interesting observation is that the self-adhesion energy W_{adh} of NBR welded in the presence of MEK continues to increase even at very long times, t_c > 24 h, when the solvent has likely

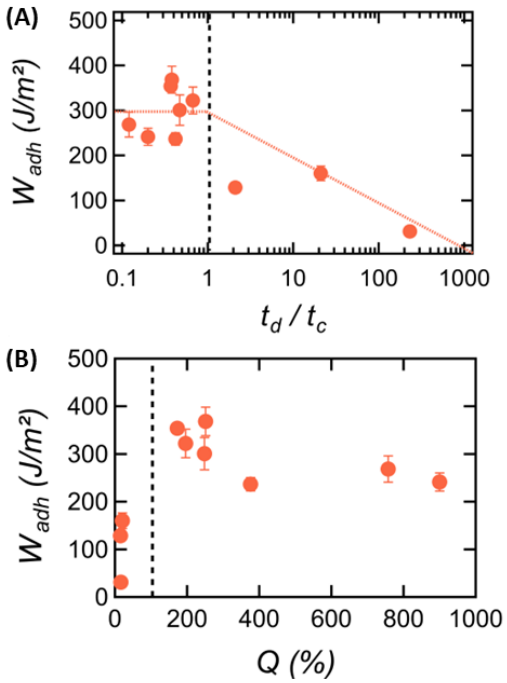

diffused away from the interface into the bulk and partially or entirely evaporated (i.e., our estimates of the solvent diffusion and evaporation timescales respectively yield $t_d \sim h_0^2/D \sim O(1\text{ h})$ and $t_e \sim R^2\phi\rho_L/4D\rho_S \sim O(100\ h)$, and are summarised in Tables S1-S2. In these scaling relations, D is the solvent diffusivity in NBR, ϕ is the equilibrium volume fraction of solvent in NBR, ρ_L is the solvent density, and ρ_S is the solvent vapour density). This observation is noteworthy because we recently demonstrated that NBR physically ages into a lamellar nanostructure of long relaxation time. Hence, the self-adhesion energy can continue to increase at $t_c \gg t_d$ and $t_c \gg t_e$ not only because of polymer interdiffusion but also because of an increasing level of microphase separation in bulk.

To further understand the role of solvent diffusion and evaporation on self-adhesion, we welded NBR with eleven solvents of different polarity for a contact time, t_c, of 3 h (Fig. 5A). Under these conditions, most solvents have sufficient time to diffuse into the bulk. However, some very polar or very non-polar solvents like methanol, isopropanol, and pentane cannot diffuse, leading to prohibitive barriers for polymer interdiffusion and negligible self-adhesion. These diffusion limitations are also reflected in the

Figure 5. Effect of solvent on the self-adhesion of NBR at fixed contact time, t_c = 3 h. Evolution of the self-adhesion energy, W_{adh}, with (**A**) the ratio of the solvent diffusion timescale, $t_d \sim h_0^2/D$, and the contact time, t_c; and (**B**) the equilibrium swelling of a cross-linked NBR, Q. Clearly, solvents that diffuse and sorb NBR afford moderate self-adhesion, $W_{adh} \approx 300$ J/m^2, comparable to that of SBR.

equilibrium swelling of a series of cross-linked NBRs (Fig. 5B), even if this is a time-insensitive thermodynamic quantity governed by the interplay between entropic elasticity and solvent-polymer mixing.

A different picture arises when the self-adhesion of NBR is not diffusion-limited and, instead, more affected by plasticisation in bulk. Under these conditions, the self-adhesion energy remains relatively constant at $W_{adh} \approx 300 \pm 50$ J/m^{2,} with variations likely arising from solvent volatility and affinity towards the polymer matrix. Hence, solvents that facilitate polymer interdiffusion and afford self-adhesion are mainly those of high diffusivity and solubility, like MEK, acetone, dichloromethane, chloroform, and toluene. However, note that though these solvents enable polymer interdiffusion, the adhesion energy, W_{adh}, is ultimately measured under conditions where the bulk progressively strengthens due to physical ageing and lamellae nanostructuring.

A final remark is that the self-adhesion energy, W_{adh}, obtained by contacting NBR at high temperatures or in the presence of tackifiers or organic solvents is comparable to that of more homogeneous, highly entangled synthetic rubbers like SBR of high molecular weight.[10] Yet, the contact time required to self-adhere is off by orders of magnitude. This observation highlights the importance of the inhomogeneous monomer distribution along the polymer chains on the large-strain mechanical properties. The blocky structure that is formed during emulsion copolymerisation of acrylonitrile and butadiene introduces drastic limitations in polymer self-diffusion due to physical associations and, in turn, results in a self-adhesive behaviour more similar to what is expected for tapered rather than random copolymers.

Conclusions

NBR is a large-volume synthetic rubber with an outstanding resistance to petrochemical fuels. This material dates back to the early 20th century when acrylonitrile and butadiene were first copolymerised by emulsion polymerisation, and today pervades the automotive and aerospace industries. However, only recently, we demonstrated that the difference in reactivity between the acrylonitrile and butadiene during emulsion copolymerisation leads to an inhomogeneous distribution of monomers along the polymer chains, as well as an ensemble of polymer chains with different compositions. As a result, NBR experiences thermodynamic driving forces for self-assembly and kinetic barriers for processing, unlike those of random copolymers and more similar to those of tapered or block copolymers.

Here, we demonstrate how such compositional drift hinders polymer interdiffusion and self-adhesion, outlining three strategies to overcome such diffusion limitations. The first is to adhere NBR notably above T_g to weaken the nanostructure and increase the molecular mobility. The second is to adhere NBR in the presence of polar tackifiers to screen the dipole-dipole interactions between acrylonitrile units. The third is to adhere NBR in the presence of organic solvents of high diffusivity and solubility. This latter strategy is noteworthy since the polymer presumably destructures and interdiffuses in the presence of organic solvent but continues to nanostructure once the solvent has evaporated to strengthen the interface and the bulk.

These strategies ultimately enable self-adhesion energies $W_{adh} \sim O(100\text{-}1000$ J/m$^2)$, comparable to those of more homogeneous copolymers such as SBR, but the interdiffusion timescales are

drastically different. Whereas SBR requires contact times, $t_c \sim O(100$ s$)$ of the order of the terminal relaxation time measured in rheology, NBR requires $t_c \sim O(100$ h$)$. This contact time is orders of magnitude larger than the reptation time of an unstructured NBR polymer. Hence, physical associations like dipole-dipole interactions, often used for toughening,[33–38] also hinder interdiffusion and self-adhesion at polymer-polymer interfaces.

Finally, we note that the investigated NBR is uncrosslinked and of industrial grade, meaning it has a strong compositional drift and a wide distribution of molecular weights. Such inhomogeneities in composition and chain length play a crucial role in the self-adhesive properties but also make the polymer physics complex. We unveil some key trends but acknowledge the need for more model systems to understand some of our results in more detail.

Author Contributions

The manuscript was written through contributions from all authors. All authors have approved the final version of the manuscript.

Conflicts of interest

There are no conflicts of interest to declare.

Acknowledgements

We thank Safran Aerosystems for supporting this work, and G.E.S. and C.C. acknowledge funding from the European Research Council (ERC) under the European Union's Horizon 2020 Research and Innovation Program (Grant Agreement No 695351 – CHEMECH).

References

1 V. Hervio, B. Bresson, A. Brûlet, I. J. Paredes, A. Sahu, V. Briand, C. Creton and G. E. Sanoja, *Macromolecules*, 2021, **54**, 2828–2834.
2 W. G. Forbes and L. A. McLeod, *Rubber Chem. Technol.*, 1959, **32**, 48–66.
3 S. S. Voyutskii and V. L. Vakula, *J. Appl. Polym. Sci.*, 1963, **7**, 475–491.
4 G. R. Hamed, *Rubber Chem. Technol.*, 1981, **54**, 576–595.
5 G. R. Hamed and C.-H. Shieh, *J. Polym. Sci. Polym. Phys. Ed.*, 1983, **21**, 1415–1425.
6 C. M. Roland and G. G. A. Boehm, *Macromolecules*, 1985, **18**, 1310–1314.
7 H. H. Kausch and M. Tirrell, *Annu. Rev. Mater. Sci.*, 1989, **19**, 341–377.
8 F. Brochard-Wyart, in *Fundamentals of Adhesion*, Springer US, Boston, MA, 1991, pp. 181–206.
9 E. Jabbari and N. A. Peppas, *J. Macromol. Sci. Part C Polym. Rev.*, 1994, **34**, 205–241.
10 R. Schach and C. Creton, *J. Rheol. (N. Y. N. Y).*, 2008, **52**, 749–767.
11 M. A. Ansarifar, K. N. G. Fuller and G. J. Lake, *Int. J. Adhes. Adhes.*, 1993, **13**, 105–110.
12 F. S. Bates and G. H. Fredrickson, *Annu. Rev. Phys. Chem.*, 1990, **41**, 525–557.
13 G. H. Fredrickson and F. S. Bates, *Annu. Rev. Mater. Sci.*, 1996, **26**, 501–550.
14 M. D. Lefebvre, M. Olvera de la Cruz and K. R. Shull, *Macromolecules*, 2004, **37**, 1118–1123.
15 M. M. Mok, J. Kim, C. L. H. Wong, S. R. Marrou, D. J. Woo, C. M. Dettmer, S. T. Nguyen, C. J. Ellison, K. R. Shull and J. M. Torkelson, *Macromolecules*, 2009, **42**, 7863–7876.
16 N. Singh, M. S. Tureau and T. H. Epps, III, *Soft Matter*, 2009, **5**, 4757.
17 A. Arrowood, M. Li, M. Nassr, N. A. Lynd and G. E. Sanoja, *Macromol. Chem. Phys.*, , DOI:10.1002/macp.202300249.
18 A. Brûlet, D. Lairez, A. Lapp and J.-P. Cotton, *J. Appl. Crystallogr.*, 2007, **40**, 165–177.
19 H. Lakrout, P. Sergot and C. Creton, *J. Adhes.*, 1999, **69**, 307–359.
20 A. Zosel, *Colloid Polym. Sci.*, 1985, **263**, 541–553.
21 A. Zosel, *J. Adhes.*, 1989, **30**, 135–149.
22 C. Creton and M. Ciccotti, *Reports Prog. Phys.*, 2016, **79**, 046601.
23 S. Poivet, F. Nallet, C. Gay and P. Fabre, *Europhys. Lett.*, 2003, **62**, 244–250.
24 F. Tanguy, M. Nicoli, A. Lindner and C. Creton, *Eur. Phys. J. E*, 2014, **37**, 3.
25 K. E. Feldman, M. J. Kade, E. W. Meijer, C. J. Hawker and E. J. Kramer, *Macromolecules*, 2009, **42**, 9072–9081.
26 L. Leibler, M. Rubinstein and R. H. Colby, *Macromolecules*, 1991, **24**, 4701–4707.
27 T. Lodge, in *Structure and Dynamics of Polymer and Colloidal Systems*, Springer Netherlands, Dordrecht, 2002, pp. 225–262.
28 S. Tang, M. Wang and B. D. Olsen, *J. Am. Chem. Soc.*, 2015, **137**, 3946–3957.
29 Z. Zhang, Q. Chen and R. H. Colby, *Soft Matter*, 2018, **14**, 2961–2977.
30 R. Schach, Y. Tran, A. Menelle and C. Creton, *Macromolecules*, 2007, **40**, 6325–6332.
31 C. Creton, E. J. Kramer, H. R. Brown and C.-Y. Hui, in *Advances in Polymer Science*, 2001, pp. 53–136.
32 J. J. Benkoski, G. H. Fredrickson and E. J. Kramer, *J. Polym. Sci. Part B Polym. Phys.*, 2002, **40**, 2377–2386.
33 C. Creton, *Macromolecules*, 2017, **50**, 8297–8316.
34 W.-C. Lin, W. Fan, A. Marcellan, D. Hourdet and C. Creton, *Macromolecules*, 2010, **43**, 2554–2563.
35 T. L. Sun, T. Kurokawa, S. Kuroda, A. Bin Ihsan, T. Akasaki, K. Sato, M. A. Haque, T. Nakajima and J. P. Gong, *Nat. Mater.*, 2013, **12**, 932–937.
36 K. Mayumi, J. Guo, T. Narita, C. Y. Hui and C. Creton, *Extrem. Mech. Lett.*, 2016, **6**, 52–59.
37 Z. S. Kean, J. L. Hawk, S. Lin, X. Zhao, R. P. Sijbesma and S. L. Craig, *Adv. Mater.*, 2014, **26**, 6013–6018.
38 J. Liu, C. S. Y. Tan, Z. Yu, N. Li, C. Abell and O. A. Scherman, *Adv. Mater.*, 2017, **29**, 1605325.